Biogeochemistry (2008) 90:171–191
DOI 10.1007/s10533-008-9243-2

Vertical distribution and chemical character of sediment phosphorus in two shallow estuaries in the Baltic Sea

K. Lukkari · M. Leivuori · H. Hartikainen

Received: 4 December 2007 / Accepted: 1 September 2008 / Published online: 14 October 2008

Abstract The vertical distribution of various phosphorus (P) forms and their relation to physico-chemical properties of estuary sediment material were studied to better understand the potential release and burial of P. Core samples were taken from two dissimilar estuaries in the Baltic Sea: one in the Archipelago Sea (AS) and one in the Gulf of Finland (GoF). The P reserves were characterized by a sequential extraction procedure including the analysis of simultaneously dissolved elements in two extraction steps. The sediment material was also analysed for particle size distribution and total elements. In addition, several environmental variables were determined. The occurrence of the various forms of P varied with sediment depth among different sites. Reductant soluble, iron (Fe) bound P was the most dynamically changing P form in the sediment, while P bound to other metal oxides and apatite-P were the most stable fractions. High sedimentation rate was a dominating factor for sediment P burial. In addition, the content of organic matter, the amount of erosion-transported sorption components, and the oxygen (O_2) conditions in the near-bottom water were important determinants of the behaviour of sediment P. The results indicate that, over the long term, both estuaries have acted as sinks for deposited P and restricted the transport of P to the AS and the open GoF, thereby partly alleviating the eutrophication process.

Keywords Baltic Sea · Fractionation · Estuaries · Phosphorus · Sediment

Introduction

Eutrophication is a severe environmental problem in many coastal sea areas around the world, including the Baltic Sea (BS). Phosphorus (P) plays a key role in this. Despite the attempts to cut down external P loading, intense algal blooms are still common in the BS (HELCOM 2003). The prevalence is ascribed to internal P load (e.g., Emeis et al. 2000): oxygen (O_2) depletion causes the reduction of iron (Fe) compounds that bind P, which leads to release of P from the sediment (Einsele 1936; Mortimer 1941, 1942). For its part, depletion of O_2 is caused by O_2 consumption in the microbiological degradation of organic matter (OM); by inflows of anoxic bottom water from the Baltic Proper; and by water column stratification, which restricts the replacement of O_2-poor near-bottom water. Vertical mixing supplies P to the productive layer enhancing algal growth. Moreover, particulate and dissolved P are continually

K. Lukkari (✉) · M. Leivuori
Finnish Institute of Marine Research,
Erik Palménin aukio 1, P.O. Box 2,
00561 Helsinki, Finland
e-mail: kaarina.lukkari@fimr.fi

H. Hartikainen
University of Helsinki, P.O. Box 27,
00014 Helsinki, Finland

transported to marine waters from terrestrial environment via rivers and estuaries.

Depending on conditions and the chemical character of P, estuaries can act as sinks or sources of P (Froelich 1988; Kamp-Nielsen 1992; Sundby et al. 1992; Forsgren and Jansson 1992, 1993). Shallowness and constant inflow of oxic water favour P retention by Fe compounds. In addition, surface sediment is oxidized through the burrowing activity of benthic fauna (e.g., Aller 1988). However, both oxic and anoxic sub-basins are typical of the sea floor of the Archipelago Sea (AS; Virtasalo et al. 2005) and the northern coast of the Gulf of Finland (GoF) (Winterhalter et al. 1981; Vallius 2006).

Sediment P can be characterized by sequential extraction where P reserves are divided into different forms according to their solubility and reactivity. In several studies on estuary sediments, P fractions have also been related to various chemical variables. Strom and Biggs (1982) concluded that P content and accumulation in the Delaware River Estuary (USA) were most closely related to reductant-soluble Fe oxyhydroxides, while calcium (Ca) phosphates existed uniformly in the sediment. They also found a positive correlation between residual P (i.e., residual organic and resistant or occluded mineral P) and OM content in the sediment. Forsgren and Jansson (1993) noticed in the River Öre Estuary (Sweden) that alkali-extractable P was high in fine-grained sediments in deep areas, while the Ca-bound P was high in shallow areas, and residual P was almost constant. In the Amazon River estuary (Brazil), Berner and Rao (1994) found a vertical decrease in deposited Fe-bound P, organic P, and total P, and explained it by desorption of oxide-bound P and liberation of P through bacterial decomposition of OM (see also Krom and Berner 1981). In the brackish water Dollard area (Wadden Sea), Fe and aluminium (Al) bound P dominated in the oxic surface sediment but decreased sharply with depth, while Ca-P was constant (Salomons and Gerritse 1981). Frankowski et al. (2002) have reported that in Pomeranian Bay (BS), Ca-bound P dominated over Fe- and Al-bound P, the sediment rich in OM was high in organic P, and occluded P was high in the surface and some deep sediment layers in the upper reach of the estuary. Contrary to this, Maher and DeVries (1994) reported that, in the Beaulieu River Estuary (England), sedimentary P was mostly associated with Fe-Al-sesquioxide phases and not related to OM.

Despite extensive research (e.g., Krom and Berner 1980, 1981; Froelich 1988; Sundby et al. 1992; Maher and DeVries 1994; Anschutz et al. 1998), the behaviour and biogeochemical processes of P in estuary and marine sediments are not fully understood. The important role of estuaries as filters and traps for river-transported P (Froelich 1988; Kamp-Nielsen 1992; Sundby et al. 1992; Forsgren and Jansson 1992, 1993), and thereby their role in reducing eutrophication of the BS, creates a need for detailed information about the nature and chemistry of P in estuary sediments.

In this study we set out to characterize the vertical distribution of various P forms in sediments of two shallow estuaries, one in the AS and one in the GoF, in relation to the sedimentation properties of the estuaries. Another aim was to assess the dependence of the P retention and release on chemical and/or physical characteristics of the sediments. This information will help clarify the contribution of the P exchange between sediment and water to eutrophication.

Materials and methods

Research area and an overview of sediment properties

The GoF is a shallow (mean depth 37 m, area 29 571 km^2) non-tidal bay in the eastern BS with stratified, low salinity water (6–10 PSU). The northern coast is indented, with a myriad of small islands, and the bottom topography is variable (Winterhalter et al. 1981).

The four sampling sites in Paimionlahti Bay (referred to later as Paila Bay, area 144.7 km^2) form a transect along the estuary starting from the inner basin of the bay and ending in a basin near the AS (south-west coast of Finland, Fig. 1). Almost half of the 1,088-km^2 drainage basin is arable land with clayey soil, while the rest is predominantly forested. Mean flow in the River Paimionjoki (length 110 km) is 10.1 m^3 s^{-1} (Kangas et al. 2003). In 1995, total P (TP), phosphate P (PO$_4$–P), and total organic carbon (TOC) loads in the Paimionjoki River were 60, 37.7, and 4,145 t a^{-1}, respectively (HELCOM 1998). The three sampling sites in the eastern GoF are located in the Ahvenkoskenlahti Bay (referred to below as Ahla

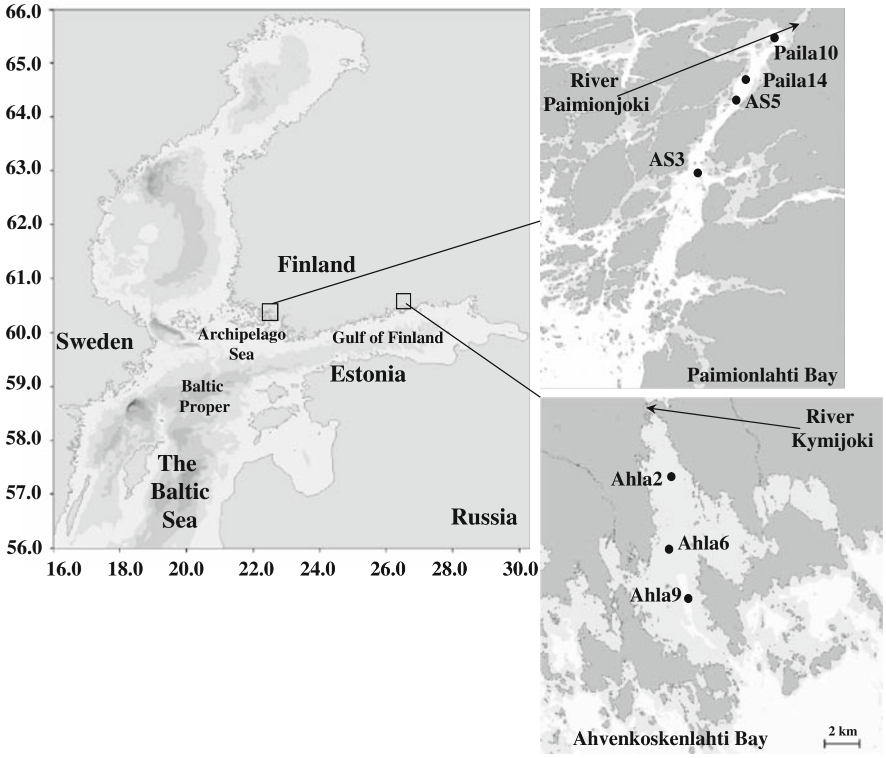

Fig. 1 The research area and location of the sampling sites in Paila Bay and Ahla Bay

Bay, area 52.5 km^2) in the vicinity of the western branch of the River Kymijoki (length ca. 200 km, Fig. 1). The drainage area of the whole River Kymijoki is 37,159 km^2, and the mean water flow in the river is 140 m^3 s^{-1}. TP, PO_4–P, and TOC loads in the River Kymijoki in 1995 were 229, 48, and 82,286 t a^{-1}, respectively (HELCOM 1998; Kangas et al. 2003).

Sediments in the study area were mainly muddy clay, rich in Fe and humic matter and poor in Ca-carbonate ($CaCO_3$). In Paila Bay, sediments had a brown, fluffy surface layer. Below that, light and dark grey and black layers alternated and occasionally were embedded with reddish brown lamina or precipitate or black sulfide spots. There were traces of bioturbation in the sediment cores. Water content in the surface of the sub-sampled 25-cm section of the sediment core was 80–85% decreasing to 70–75% at 10 cm depth. In their main features the sediment profiles in Ahla Bay were similar to those in Paila Bay, but traces of bioturbation were more abundant in the sediment and water content ranged from 80 to 90% in the sub-sampled 25-cm section.

Sampling

Sediment samples were collected on two cruises of r/v Aranda (assisted by r/v Aurelia and r/v Muikku): at the end of August in 2003 (Paila Bay: sites Paila10, Paila14, AS3, and AS5) and 2004 (Ahla Bay: sites Ahla2, Ahla6, and Ahla9). The samples were taken with a Gemax gravity corer (two acrylic cylinders, inner diameter 9 cm, length ca. 60 cm). The cores were put vertically on a slicing table and covered with a glove bag tightly joined to another glove bag. The glove bags were sealed and filled with nitrogen (N_2, purity 99.5%) until O_2 content was <5–10% (detected with Gas Alert detectors calibrated against fresh air, O_2 content 20–21%). After the water column above the sediment (5 cm) had been sampled and the rest of the near-bottom water removed by gradually lifting the sediment core inside the cylinder with a piston, the core was cut into 1-cm slices (0–10, 14–15, 19–20, and 24–25 cm depth intervals in Paila Bay and 0–3, 4–5, 6–7, 9–10, 14–15, and 24–25 cm depth intervals in Ahla Bay). Sectioning was made by holding a small cylinder of same diameter on top of the cylinder of the corer, lifting the sediment gradually upwards with the piston, and pushing (horizontally) a thin plastic plate between the two cylinders. The 1-cm sediment section, which was cut into the upper cylinder, was pulled along the plate and dropped into a sediment container. The samples of two parallel cores were pooled and sealed in plastic containers in the second glove bag (cooled with ice, $O_2 < 5\%$), and the containers were vacuum packed (Tecla s.n.c Vacum 33) into gas-tight plastic bags (N_2 as shielding gas) and stored at 5°C (in dark) until analysis. According to our previous study, storing sediment samples in N_2-atm at 5°C has relatively little effect on P fractions (Lukkari et al. 2007a). Cores from Paila10 and Ahla Bay were transported with the smaller vessels to r/v Aranda for sub-sampling. The cores were capped, cooled with ice, and protected from light during the transport.

Analytical methods

Water column and pore water samples

Water column salinity, temperature, and dissolved O_2 were determined with a CTD instrument (Sea-Bird Electronics SBE 911plus, Sea-Bird Electronics SBE 13 for O_2). Dissolved P (PO_4–P), nitrate (NO_3–N), ammonium (NH_4–N), and silicate (Si) as well as total P (TP) and N (TN) (after acid persulfate digestion) were determined onboard with a spectrophotometer (Lachat QuickChem 8000 autoanalyser) by methods described in Hansen and Koroleff (1999). Dissolved O_2 in the near-bottom water (ca. 5 cm above the sediment) was determined by Winkler titration (Grasshoff 1983). The near-bottom water was analysed for dissolved (filtered with Nuclepore polycarbonate (PC) membranes, pore size 0.4 μm) and total (unfiltered) nutrients as above. For study of the incubation-derived PO_4–P flux, four intact replicate sediment cores were incubated at in situ temperature (in dark, continuously gently stirring the water column), and PO_4–P concentration was determined at the beginning and after 5-h incubation. The PO_4–P flux was calculated per surface area on the basis of the concentration difference in the beginning and after the incubation. Determination of dissolved O_2 in a pre-experiment showed that oxic cores did not get anoxic during the 5-h incubation (H. Haahti, FIMR, pers. com.).

Sediment pore water (up to ca. 4 cm depth) was collected in argon (Ar) atmosphere (atm) using a whole-core hydraulic squeezer (Bender et al. 1987; Mäkelä and Tuominen 2003) from sites Paila14, AS5, AS3, and Ahla9. In this method, the sampling interval (in mm) is calculated from the porosity of the sediment, the volume of collected pore water, and the radius of the cylinder of the corer (Bender et al. 1987; Mäkelä and Tuominen 2003). The problems caused by the method for particle-reactive species (Bender et al. 1987) were reduced by starting the sampling immediately after lifting the core and using Ar atm shielding. Pore water was analysed on board for dissolved (pore size 0.45 μm) nutrients. Portions of the pore water samples that had been acidified (65% s.p. HNO_3, pH < 2, storage at 5°C) were later analysed for total dissolved Fe and manganese (Mn) by ICP-AES.

Sediment

A pair of sediment cores was sectioned (at the same intervals, without N_2 atm) and the samples were immediately frozen (−18°C) and later freeze-dried and homogenized (Pulverisette 5) for total analysis of P (TP_{sed}), Fe, Mn, Al, and Ca. The elements were measured with an ICP-AES (TJA-25, Thermo Jarrell Ash) after digestion with combined fluoric acid, aqua regia, and boric acid in a microwave oven (CEM-205). The procedure follows the method accredited for determination of Al, Mn, and Fe in the laboratory of FIMR (Leivuori 2000, modified from Loring and Rantala 1992). In the reference materials, i.e., Buffalo River sediment 8704 (not certified for P) and MESS-3 (NRCC, informative value for P only), the recovery of P varied between 96 and 112% and the recoveries of Ca, Fe, and Al between 88 and 108%. Detection limit for TP_{sed} was 5 μg g^{-1} (0.16 μmol g^{-1}).

Redox potential, pH, and temperature were determined from one core by slowly pushing electrodes (SenTix Sur for pH, SenTix ORP for redox, and TFK325 for temperature; all jointed to the same device) into the sediment. The measurement was started at about 5 cm above the sediment and continued into the sediment at 1-cm intervals until about 10 cm depth. The surface material was removed to reach the deeper layers. Electrodes were calibrated with commercial buffer solutions, and the redox potential values were converted to standard hydrogen electrode values (E_h) after temperature correction following the manufacturer's instructions. Sometimes sediments contain hydrogen sulfide, which is deleterious for common electrodes; thus, the redox potentials determined in this study are considered descriptive only.

^{137}Cs activity was determined in the laboratory of the Finnish Radiation and Nuclear Safety Authority (according to Kyzyurov et al. 1994; Kankaanpää et al. 1997; Mattila et al. 2006) for sediment dating and calculation of sediment accumulation rate estimates (SAR values). Within the research area, ^{137}Cs peak values indicate sediment deposition in 1986 (the fallout following the Chernobyl accident). SAR values for some of the sites are published in Mattila et al. (2006). Particle size distribution was determined at the Geological Survey of Finland (GTK) by sieving (particles Ø > 60 μm) and with a Sedigraph analyser (Ø < 60 μm). Total carbon (TC), organic carbon (TOC), nitrogen (TN), and sulfur (TS) were determined with a LECO CNS-2000 analyser in the laboratory of the Pirkanmaa Regional Environment Centre. GTK provided sediment profile descriptions.

P fractionation

In the P fractionation procedure (Table 1), fresh sediment equivalent to 0.50 g of dry matter (DM) was extracted and rinsed with 50.0 ml of solutions mainly following the scheme of Jensen and Thamdrup (1993), which is modified from the procedure of Psenner et al. (1984). The Jensen and Thamdrup (1993) method was slightly modified further by replacing step V with the corresponding step in SEDEX-method by Ruttenberg (1992). A detailed description of the extraction and working practices is given in Lukkari et al. (2007b). Briefly, in step I, NaCl removes loosely adsorbed and pore water P (referred to later as NaCl-iP). In step II, NaBD (at pH 7) extracts redox-sensitive P bound to hydrated oxides of reducible metals, mainly Fe (NaBD-iP). In step III, NaOH extracts P bound to oxides of metals not reduced in the previous step (e.g., Al; NaOH-iP) and the labile organic P, NRP. The term NRP, i.e., “non-reactive P” indicates that these organic P compounds don’t react in molybdate-blue method used in determining PO_4–P. In step IV, HCl dissolves Ca-bound P, mainly from apatite minerals (HCl-iP). Steps I-IV include one or two rinsing steps to reduce matrix effect and tailing, and steps I-II were extracted in N_2-atm in a glove box to avoid oxidation of the sediment. In step V, the sediment residues are dried (24 h at 105°C), combusted, and extracted with HCl to determine residual P (Res-P), i.e., the refractory organic P. Filtered (Nuclepore PC membranes, pore size 0.4 μm) extracts were analysed for dissolved PO_4–P and unfiltered extracts for TP (dissolved PO_4–P after acid persulfate digestion, Koroleff 1983). The filtered and acidified extracts in steps II and III were also analysed for total dissolved (T_{diss}) Fe, Mn, Al, Ca, Mg, and Si by ICP-OES in the Institute for Environmental Research at the University of Jyväskylä. Elemental composition is presented only for NaBD- and NaOH-extracts, because these were the most interesting extracts considering binding of P. The elemental composition of all extracts with respect to P sources was discussed in our previous work (Lukkari et al. 2007b).

Jensen et al. (1995) roughly divided the P fractions into mobile and immobile P: the mobile P fraction includes NaCl-iP, NaBD-iP, and NRP and the immobile P fraction NaOH-iP, HCl-iP, and Res-P. In our modification, however, the particulate (>0.4 μm) part of the NRP in NaOH is included in Res-P, and only the dissolved (<0.4 μm) part is included in the NRP fraction. Furthermore, because in several studies the part of sediment P, which is available for bacteria or

Table 1 Outline of the P fractionation scheme

Step	Extractant	Separated P fraction
I	0.46 M sodium chloride (NaCl), 1 h	Pore water P, loosely sorbed P (NaCl-iP)
II	0.11 M sodium dithionite in sodium bicarbonate, pH 7 (NaBD), 1 h	P bound to oxides of reducible metals (Fe and Mn) (NaBD-iP)
III	0.1 M sodium hydroxide (NaOH), 18 h	P from Al oxides, non-reducible Fe compounds (NaOH-iP) and labile organic P (NRP)
IV	0.5 M hydrochloric acid (HCl), 1 h	Apatite and other inorganic P (HCl-iP)
Ignition of the sediment residue: 2 h at 550°C		
V	1 M hydrochloric acid (HCl), 16 h	Residual, mainly refractory organic P (Res-P)

algae, or undergoes changes and diagenetic transformations in the sediment (degradation, sorption, desorption, dissolution, or precipitation) is termed “reactive P” (Froelich et al. 1982; Froelich 1988; Louchouarn et al. 1997; Delaney 1998; Anderson et al. 2001), we chose to use “reactive P” instead of “mobile P”. It is noteworthy that the sedimentary reactive P differs from “dissolved reactive” or “molybdate-reactive” P (i.e., PO_4–P) in solution. Jensen and Thamdrup (1993) divided organic P into two fractions, labile (NRP) and refractory (Res-P). In this rough division, the former is considered reactive P form, while the latter is considered immobile P form. Burial fluxes for P were calculated by multiplying the immobile P (see discussion) in the surface layer by the SAR values. The burial efficiency of P was expressed as the portion of immobile P in the surface as percentage of the total extractable P (TP_{extr}), i.e., the sum of P in the separate fractions (Jensen et al. 1995). The long-term average for the annual efflux of sediment P was calculated from the concentration difference between reactive P in the surface layer and at the nearest sample depth to the ^{137}Cs maximum (i.e., year 1986) at each site, and dividing that by the age difference (in years).

Statistical analyses

Statistical analyses were mostly carried out using the mixed model, run with the Statistical Analysis System (SAS) program, to determine which variables (elements in sediments and extracts) explain the different P fractions. The mixed model is one type of models used in variance analysis and it includes both fixed and random variables. The mixed model was chosen because, in this study, observations were correlated, i.e., different variables were determined from several depth layers at each sampling site. The sampling site was set as a random variable, and the sediment depth layer was treated as a repeated factor (autoregressive structure in the longitudinal data assumed). The dependence in the mixed model was tested with F-test and considered significant when ≤ 0.050. Parameters for the mixed model analysis were chosen on the basis of their mutual relationships, which were studied with the Pearson correlation with Bonferroni probabilities, considering probability <0.0001 statistically significant. Another approach was principal components analysis (PCA, with Varimax rotation) carried out on the basis of Spearman correlations (variables did not follow bivariate normal distribution). PCA was considered advantageous because of the high number of variables that were correlated with each other. In PCA, parameters determined from sediment were treated as variables explaining the P fractions.

Results

Water column and pore water

Parameters describing the near-bottom water are presented in Table 2. All sites except AS5 were oxic (dissolved $O_2 > 2$ ml l^{-1}), but the near-bottom water PO_4–P was higher at Ahla6 and Ahla9. The incubation-derived PO_4–P flux was determined at four sites, and at three of them (Paila14, AS3, and Ahla9) the flux was directed from sediment to water even though the near-bottom water was oxic. This positive PO_4–P flux was clearly highest at Ahla9 and lowest at AS3. A negative flux was measured at AS5 even though the site was hypoxic ($O_2 < 2$ ml l^{-1}). The salinity in Paila Bay was 6.1–6.3 PSU, and higher than the values reported for Ahla Bay (4–5 PSU) by Kangas et al. (2003).

Small panels on the right in Fig. 2a and b show that pore water NH_4–N, PO_4–P, and NO_3–N generally increased with sediment depth. Of the three outermost sampling sites of Paila Bay, PO_4–P was lowest at AS3 (0.3–14.1 µmol l^{-1}) and increased gradually towards the inner estuary, varying between 2.6 and 11.1 µmol l^{-1} at AS5 and between 5.9 and 50.4 µmol l^{-1} at Paila14 (Fig. 2a). At Ahla9, it was many times higher (4.5–531 µmol l^{-1}; Fig. 2b). Ahla9 also exhibited the highest NH_4–N and the lowest NO_3–N concentration. At all sites, dissolved Fe and Mn increased with sediment depth and values were highest at AS5 (60.2–248 µmol l^{-1} for Fe and 52.4–110 µmol l^{-1} for Mn) and lowest at AS3 (21.5–73.6 µmol l^{-1} for Fe and 8.4–74.6 µmol l^{-1} for Mn).

Sediments

Split cores revealed the heterogeneity of the sediment. Bioturbation was evident at all sites, and the sporadic occurrence of Fe-rich reddish brown laminas and black sulfide layers or spots has generated variation in the vertical distribution of the elements. The elemental composition of the sediment profiles is presented in Table 3. Total carbon (TC) consisted almost entirely

Table 2 Parameters describing properties of the sampling sites and near-bottom water

Parameter	Paila10	Paila14	AS5	AS3	Ahla2	Ahla6	Ahla9
Water depth (m)	12	29	33	19	4	7	13
Distance from shore (m)	4	10	12	20	5	8	10
Near-bottom water							
O_2 (ml l^{-1})	6.2 *	2.9	1.7	6.1	6.4 *	4.3 *	4.5
PO_4^{3-} (µmol l^{-1})	0.4	0.7	0.9	0.3	0.9	1.6	2.9
TP (µmol l^{-1})	1.8	2.5	3.2	3.2	2.3	2.9	4.0
SiO_4–Si (µmol l^{-1})	20.4	23.7	27.7	14.3	24.1	19.3	21.7
NO_3–N (µmol l^{-1})	0.4	7.6	14.1	1.5	3.6	3.1	3.6
NH_4–N (µmol l^{-1})	5.1	7.7	7.2	2.3	8.5	8.6	10.8
TN (µmol l^{-1})	33.6	45.1	41.4	44.1	37.9	47.8	34.7
PO_4–P flux (µmol m^{-2} d^{-1})	–	+278	−4.2	+24.4	–	–	+671
Salinity (PSU)	–	6.2 *	6.3 *	6.3 *	–	–	–
Temperature (°C)	14.3	13.6	10.7	13.4	17.3	11.9	8.4
pH	7.5	6.3	6.9	7.2	7.5	7.1	7.5
E_h (mV)	349	320	348	350	359	311	366

Values labelled with an asterisk (*) were determined ca. 1 m above the sediment

of organic C (OC; about 95%) and varied from 1,618 to 4,658 µmol g^{-1} DW, decreasing with sediment depth. Total nitrogen (TN; range 112–435 µmol g^{-1} DW), total sulfur (TS; range 45.3–424 µmol g^{-1} DW), and especially TC were higher in Ahla Bay than in Paila Bay. TN clearly decreased with sediment depth, while TS mainly increased. TP_{sed} (range 26.9–107 µmol g^{-1} DW) generally decreased with depth, and peak concentrations were recorded at Ahla9. As for the metals, Al and Fe were present in higher concentrations in Paila Bay than in Ahla Bay. Neither Al (range 2,323–4,247 µmol g^{-1} DW) nor Fe (range 571–1,579 µmol g^{-1} DW) showed a clear trend with sediment depth. Mn was low (range 7.4–19.9 µmol g^{-1} DW) and did not show either vertical or spatial trends. In contrast to this, a decreasing vertical trend was found for Ca (range 174–351 µmol g^{-1} DW).

At all sites, clay (<2 µm) was the dominating particle size fraction. Its proportion was higher in Paila Bay than in Ahla Bay (Fig. 3). Redox potential in the near-bottom water (Fig. 4) varied between +311 and +366 mV at all sites. In the sediment, the redox potential strongly decreased within the first 1–2 cm. The surface sediment of Ahla6 was most reduced, while that at Ahla2 was most oxidized. pH in the near-bottom water (Fig. 4) varied between 7.5 (Ahla9) and 6.3 (Paila14), and typically the decreasing trend in the surface sediment was followed by a slightly increasing trend. Temperature at the sediment surface in Paila Bay ranged between 11 and 13.5°C.

Fig. 2 (**a**) Vertical distribution of different P fractions in sediments in Paila Bay. The *y*-axis represents sediment depth in cm and the *x*-axis represents concentration of P in µmol g^{-1} DW. Differences between triplicate or duplicate samples were <0.2, <2.7, <1.8, <1.8, and <1.1 µmol P g^{-1} DW for fractions NaCl-iP, NaBD-iP, NaOH-iP, HCl-iP, and Res-P, respectively. The dotted line shows the evaluated depth of the peak ^{137}Cs value (i.e., the year 1986). The panel on the right represents dissolved nutrients (PO_4–P, NO_3–N, and NH_4–N) and metals (Fe and Mn) in the sediment pore water. The *y*-axis represents sediment depth in cm. The *x*-axis represents concentration in µmol l^{-1}. (**b**) Vertical distribution of different P fractions in sediments in Ahla Bay. The *y*-axis represents sediment depth in cm and the *x*-axis represents concentration of P in µmol g^{-1} DW. Differences between duplicate samples were <0.1, <0.9, <0.5, <0.4, and <0.3 µmol P g^{-1} DW for fractions NaCl-iP, NaBD-iP, NaOH-iP, HCl-iP, and Res-P, respectively. The dotted line shows the evaluated depth of the peak ^{137}Cs value (i.e., the year 1986). The panel on the right represents dissolved nutrients (PO_4–P, NO_3–N, and NH_4–N) and metals (Fe and Mn) in the sediment pore water. The *y*-axis represents sediment depth in cm. The *x*-axis represents concentration in µmol l^{-1} ▶

P fractions

The fractionation procedure extracted on average 90% of TP_{sed}. In the two areas taken together about 22–50% of TP_{extr} was organic and 50–77% inorganic. The portion of organic P was highest at the outermost

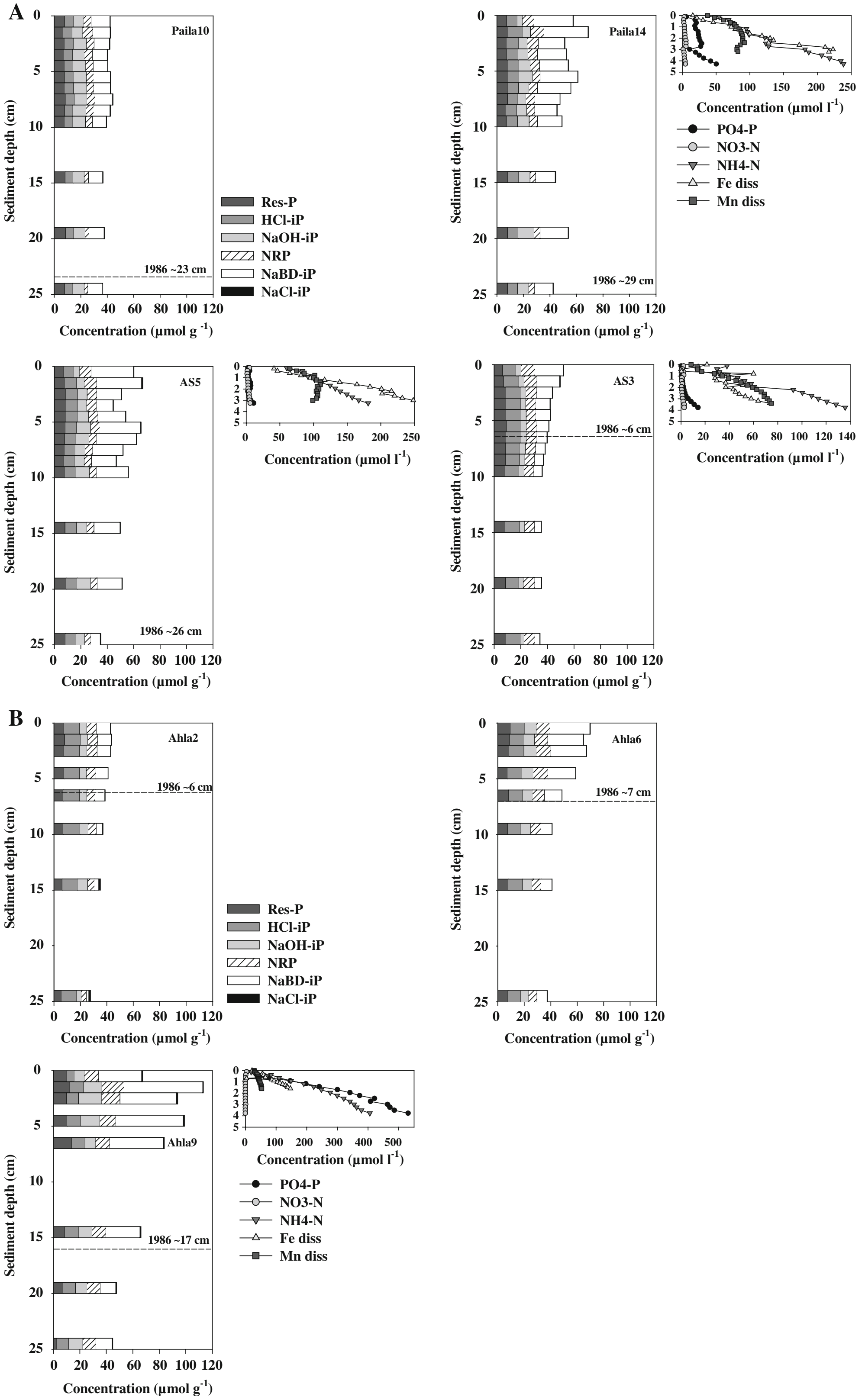
A
B
Paila10
Paila14
AS5
AS3
Ahla2
Ahla6
Ahla9
1986 ~23 cm
1986 ~29 cm
1986 ~26 cm
1986 ~6 cm
1986 ~6 cm
1986 ~7 cm
1986 ~17 cm
Sediment depth (cm)
0
5
10
15
20
25
Concentration (µmol g-1)
0 20 40 60 80 100 120
Concentration (µmol l-1)
0 50 100 150 200 250
0 20 40 60 80 100 120 140
0 100 200 300 400 500
Res-P
HCl-iP
NaOH-iP
NRP
NaBD-iP
NaCl-iP
PO4-P
NO3-N
NH4-N
Fe diss
Mn diss

Table 3 Total concentrations of P, C, N, S, Fe, Mn, Al, and Ca in sediment depth profiles. The concentrations are presented in μmol g^{-1} DW

cm	P	C	N	S	Fe	Mn	Al	Ca	P	C	N	S	Fe	Mn	Al	Ca
	Paila10								Paila14							
1	47.2	2,024	188	65.9	1,139	13.1	3,544	218	76.1	2,555	230	122	1,393	17.9	3,910	243
2	45.4	1,998	181	64.2	1,282	13.2	2,690	199	71.7	2,813	256	174	1,263	17.9	3,005	233
3	42.9	1,990	164	68.2	1,279	11.9	2,643	351	61.5	2,455	219	124	1,579	19.9	3,247	216
4	46.2	1,965	158	72.5	1,090	11.9	3,505	216	61.6	2,338	194	107	1,464	16.7	3,437	220
5	45.1	1,957	166	79.0	1,094	11.0	3,318	199	57.3	2,289	189	98.1	1,051	13.3	3,467	234
6	46.5	1,928	156	67.3	1,095	10.8	3,754	217	69.7	2,108	170	93.9	1,193	15.9	3,296	201
7	49.5	1,884	151	57.7	1,241	10.9	3,642	228	74.9	2,089	173	107	1,525	15.5	3,305	210
8	44.6	1,854	157	49.9	1,159	9.9	3,347	200	63.5	2,068	172	106	1,470	15.4	3,851	214
9	54.6	1,839	140	46.1	1,143	11.0	3,747	205	55.5	2,079	171	95.4	1,462	15.7	3,751	213
10	45.8	1,814	138	45.3	1,042	9.7	2,650	203	54.7	2,062	160	101	1,231	11.3	3,004	222
15	51.8	1,723	126	72.0	1,440	11.5	4,247	209	52.1	2,073	170	123	1,319	12.3	4,088	200
20	43.6	1,669	112	105	1,062	10.5	3,951	183	50.0	2,032	192	143	1,210	12.7	3,579	191
25	40.6	1,618	112	135	1,230	12.3	3,351	174	42.5	1,977	169	193	1,328	12.2	3,832	198
	AS5								AS5							
1	67.8	2,763	355	149	1,087	13.7	2,848	257	59.0	2,952	243	105	947	11.9	3,020	292
2	66.4	2,836	379	134	1,044	15.6	2,419	243	54.9	2,915	342	91.2	1,008	11.2	3,184	276
3	52.0	2,691	327	137	1,137	13.5	3,385	233	48.6	2,855	338	85.5	956	11.0	3,266	292
4	57.3	2,481	298	118	1,467	15.0	3,843	272	49.8	2,812	323	85.9	943	10.9	3,131	240
5	62.6	2,373	272	103	1,091	13.5	3,452	210	48.6	2,758	320	94.3	966	11.3	3,048	244
6	73.6	2,164	252	104	1,125	13.5	3,355	192	46.9	2,754	315	124	968	11.2	3,202	252
7	88.3	2,258	246	133	1,439	16.0	4,062	184	40.4	2,695	297	168	983	10.5	3,329	225
8	60.6	2,244	255	123	1,109	12.3	2,895	191	47.2	2,688	324	188	1,087	12.1	3,213	231
9	62.1	2,185	265	97.1	1,186	14.9	3,517	210	39.4	2,659	301	210	1,041	11.0	2,800	219
10	53.4	2,190	245	116	1,313	15.2	3,168	229	40.3	2,632	292	232	999	10.8	3,042	232
15	47.6	2,192	250	123	1,328	16.1	2,323	258	41.6	2,440	269	214	1,110	12.6	2,800	234
20	52.5	2,104	254	139	1,200	14.1	2,826	206	39.8	2,300	259	199	1,073	13.3	2,478	235
25	38.6	2,187	236	195	1,034	12.3	3,678	212	40.2	2,159	238	192	1,075	14.4	2,413	245
	Ahla2								Ahla6							
1	41.3	4,450	321	112	601	9.9	2,497	245	76.3	4,138	314	150	830	11.8	2,869	291
2	47.7	4,488	293	103	707	10.6	2,927	297	69.4	4,213	318	134	771	10.6	2,753	248
3	47.7	4,467	289	103	748	10.5	3,051	296	69.3	4,167	314	140	930	12.4	2,999	280
5	49.2	4,517	289	111	720	9.5	2,950	276	70.7	4,134	303	159	865	11.5	2,659	231
7	42.1	4,504	286	133	737	9.3	2,789	281	50.7	4,113	289	246	832	10.4	2,977	242
10	36.6	4,567	246	268	603	7.4	2,675	247	41.4	4,204	264	341	744	12.1	2,903	234
15	35.6	4,658	218	313	687	8.2	2,836	256	39.3	4,121	243	324	815	12.7	2,945	217
25	26.9	3,755	175	424	723	8.3	2,572	243	37.4	3,688	200	421	1,028	18.7	3,393	260
	Ahla9															
1	93.1	4,429	436	168	813	16.1	2,597	239								
2	107	4,517	425	187	816	16.2	2,582	229								
3	90.9	4,413	393	131	803	17.1	2,768	216								
5	101	4,313	386	271	1,010	18.9	3,145	227								
7	88.8	4,063	336	158	886	16.1	3,090	245								
10	76.6	4,000	321	204	571	13.1	2,844	212								
15	43.9	4,146	311	278	743	11.2	2,676	202								
25	40.6	4,125	268	318	699	11.8	2,796	177								

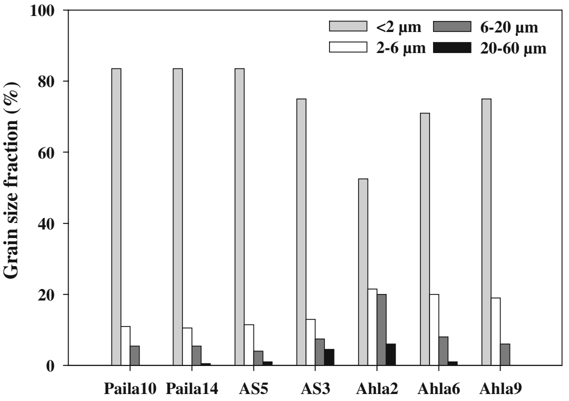

Fig. 3 Particle size distribution in the surface sediment (0–1 cm) of each sampling site. The *y*-axis represents percentual (per weight) portion of each size fraction

site, 20 m from the shore (AS3). The vertical distribution of TP_{extr} varied markedly (Fig. 2a, b). At Paila10 and Ahla2 it was more or less homogeneous, while at Paila14 and AS5 it fluctuated strongly with sediment depth.

Vertical profiles of the P fractions (Fig. 2a, b) revealed the dominating role of reductant soluble P: the portion of NaBD-iP of TP_{extr} tended to be largest in the oxic surface layers (25–53%), but a considerable part was also found in the deepest layers. NaBD-iP was highest at Ahla9, where it also showed the largest vertical variation (1.8–59.4 µmol g^{-1} DW). At the innermost sites of the bays, NaBD-iP was either fairly stable or fluctuating, while at the outermost sites it decreased with sediment depth. NaOH-extractable organic P, NRP, constituted 9–24% of TP_{extr}. Quantitatively NRP was highest at the organic-rich site Ahla9 (16.8 µmol P g^{-1} DW), but the portion of NRP of TP_{extr} was highest at AS3. The pore water P (NaCl-iP) was very low (usually <1% of TP_{extr}), and 1.3 µmol P g^{-1} DW at maximum (at 25-cm depth at Ahla2).

The immobile inorganic P was dominated by apatite-P (HCl-iP, range 5.9–12.7 µmol P g^{-1} DW, 9–42% of TP_{extr}), which also showed the smallest vertical variation within all profiles. Apatite-P was the major P fraction at the outermost site of Paila Bay (AS3) and even more dominant at the shallowest site in Ahla Bay (Ahla2). P bound to oxides of metals not reduced chemically (NaOH-iP) constituted 7–24% of TP_{extr} (range 3.1–17.5 µmol P g^{-1} DW). The absolute amount was greatest at Ahla9, but relatively NaOH-iP was greatest at Paila10. The refractory organic P (Res-P, 6–27% of TP_{extr}) showed the smallest spatial variation (range 2.7–14.1 µmol P g^{-1} DW). It is noteworthy in Paila Bay that, when going from the inner towards the outer estuary, the portions of apatite-P and NRP increase and those of P bound to metal oxides decrease.

The SAR values, sedimentation of TP_{extr}, burial of the immobile P, burial efficiency of deposited P, and the long-term average values for P efflux are presented in Table 4. The SAR values varied greatly, being highest at the three innermost sites of Paila Bay followed by Ahla9. The amounts of deposited P (in mmol m^{-2} y^{-1}) were highest at Paila14 and AS5 that also had highest SAR values.

Total elements in NaBD- and NaOH-extracts

NaBD extracted Fe considerably more than NaOH (Table 5) and Fe showed a declining trend in NaBD with sediment depth. NaBD-extractable Fe (NaBD-Fe) was highest in surface sediment layers in Paila Bay, which were also rich in NaOH-Fe. NaOH

Fig. 4 Redox potential and pH in the near-bottom water and at the sediment surface. The *y*-axis represents sediment depth in cm (0 is the sediment surface, negative values are in the sediment). The *x*-axis represents E_h in mV or pH. The dotted line in the E_h figure represents +230 mV

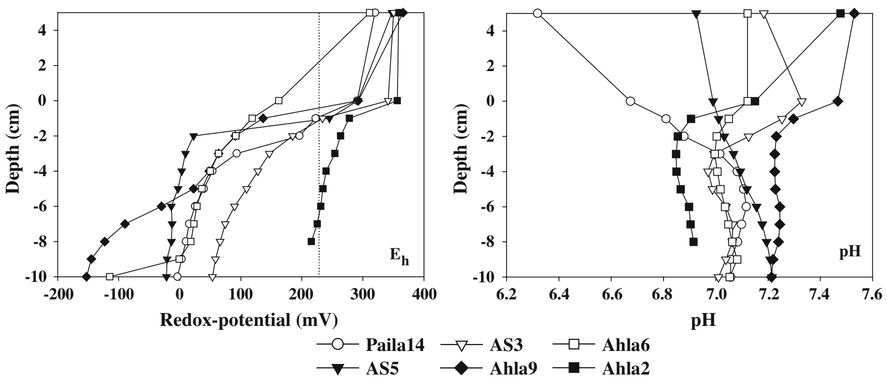

Table 4 Sediment accumulation rates (SAR), sedimentation of extractable P, burial fluxes of immobile P, long-term average for P efflux, and burial efficiency of P at different sites

Site	SAR	Sedimentation of P		Burial of P		Long-term aver. efflux of P		Burial efficiency (%)
	g m^{-2} y^{-1}	mmol m^{-2} y^{-1}	g m^{-2} y^{-1}	mmol m^{-2} y^{-1}	g m^{-2} y^{-1}	mmol m^{-2} y^{-1}	mg m^{-2} y^{-1}	
Paila10	4,580*	193	6.0	165	5.1	1.7	51.3	85
Paila14	5,540*	319	9.9	209	6.5	6.5	200	66
AS5	4,650*	280	8.7	146	4.5	7.9	244	52
AS3	840*	43.9	1.4	31.3	1.0	0.7	22.9	71
Ahla2	730	31.3	1.0	28.2	0.9	0.2	5.3	90
Ahla6	660	46.1	1.4	33.9	1.1	0.7	21.0	74
Ahla9	1,373	92.6	2.9	62.7	1.9	1.7	51.5	68

SAR values labelled with an asterisk (*) are presented in Mattila et al. (2006)

extracted most Al at the two innermost sites of Paila Bay. The amount of Al in NaBD-extract was negligible. Both extracts were relatively low in Mn, Ahla9 being the site richest in NaBD-Mn. The alkaline earth metals, Mg and Ca, were present in low concentration in NaOH and NaBD fractions. NaOH extracted Si considerably more than NaBD. NaOH-Si was highest at Ahla6 and Ahla9, and in both estuaries it was lowest at the innermost sites.

Statistical analyses

Since the age of the sediment profiles varied widely, the results obtained from different depth layers were pooled into five age classes on the basis of the ^{137}Cs dating and assuming a constant sediment accumulation over time. In the mixed model analysis, P fractions (except NaCl-iP) were usually related to the age class. Other significant relationships are presented in Table 6. In the PCA (run only for the Paila Bay data), three factors (i.e., components) were formed (Eigenvalues > 1, total variation explained >14%). Phosphorus fractions NaOH-iP, NRP, and HCl-iP were loaded to factor 1 (with sediment C, N, Al, and Ca). NaBD-iP was loaded to factor 2 (with sediment P, Mn, and Fe), and NaCl-iP was loaded to factor 3 (with sediment TS). Res-P was divided between factors 2 and 3. The correlation analysis (all depth layers were included) revealed several correlations between the P fractions and elements in the sediments and the extracts. Meaningful positive correlations were those found between NaOH-extractable inorganic P and Al as well as between NaBD-soluble Si and Al. Positive correlation was also found between NRP and sediment TC and TN. NaOH-iP correlated negatively with NRP and HCl-iP, and HCl-iP also correlated negatively with NaOH-Al.

Discussion

Sediment properties

The SAR values (Table 4) clearly show that sedimentation has been much slower in Ahla Bay than in Paila Bay, where the inner estuary seems to act as a trap for material transported from the watershed. The Ahla Bay sediment was richer than the Paila Bay sediment in OM (TC) (coinciding with the higher TOC load in the River Kymijoki than in the River Paimionjoki; HELCOM 1998, see the description of the research area), while the Paila Bay sediment was richer than the Ahla Bay sediment in TFe_{sed}, TAl_{sed} (Table 3), and clay material. In Ahla Bay, the portion of the clay size fraction increased outwards (Fig. 3). Despite the lower SAR, P accumulation has been higher in Ahla Bay than in Paila Bay (Fig. 2a, b), perhaps due to the higher water flow and TP load carried by the River Kymijoki (HELCOM 1998; Kangas et al. 2003).

Vertical distribution of P and other extracted elements

The dominant influence of sediment accumulation on P distribution in the sediments was evident: in general, the higher the SAR value (Table 4) the greater was the variation in vertical distribution of sediment P (Fig. 2a, b). In inner parts of the estuaries (Paila10 and Ahla2), the vertical distribution of TP_{extr} was

Table 5 Total concentrations of dissolved elements extracted along with P in NaBD and in NaOH. All concentrations are presented as μmol g^{-1} DW

Depth (cm)	NaBD						NaOH						NaBD						NaOH					
	Mg	Si	Al	Ca	Mn	Fe	Mg	Si	Al	Ca	Mn	Fe	Mg	Si	Al	Ca	Mn	Fe	Mg	Si	Al	Ca	Mn	Fe
	Paila10												Paila14											
1	[a]	4.6	0.8	4.3	1.9	129	[a]	303	173	0	0.1	14.5	[a]	6.8	1.5	5.8	3.2	152	[a]	325	110	0	0	1.2
2	[a]	5.4	1.0	5.4	1.8	106	[a]	340	211	0.7	0.4	48.4	[a]	11.6	3.1	9.9	5.5	84.5	[a]	429	127	0	0.1	7.5
3	8.3	5.4	0.4	5.5	1.4	32.2	0.5	278	159	0	0	2.2	[a]	17.9	7.8	4.8	3.1	56.6	19.1	386	157	0.3	0.3	37.2
4	7.8	5.7	0.6	5.2	1.1	24.2	1.6	277	159	0	0	4.6	[a]	17.4	8.7	2.6	2.0	79.0	14.1	369	160	0.3	0.2	27.1
5	6.5	5.7	0.5	4.4	0.9	36.1	2.1	275	165	0	0	6.0	[a]	5.9	1.2	3.7	2.7	61.1	3.8	340	140	0	0.1	9.0
6	6.1	5.9	0.7	4.6	0.9	57.6	2.3	271	167	0.1	0	6.2	[a]	6.7	1.2	3.3	1.8	81.5	0	326	129	0	0	1.6
7	7.1	5.8	0.9	5.1	0.8	64.8	1.7	269	170	0	0	5.2	[a]	8.1	1.2	3.4	1.6	55.0	1.4	339	134	0	0	4.0
8	6.6	7.0	0.9	4.7	0.8	44.1	0.7	279	150	6.8	0	2.0	[a]	7.8	1.2	3.1	1.2	57.5	2.8	327	134	0	0	6.6
9	6.6	6.5	0.9	5.5	0.7	43.0	0.2	296	189	0.2	0.1	16.1	5.6	6.9	0.6	4.5	2.0	16.8	4.5	324	135	0	0.1	10.0
10	5.9	6.5	1.2	4.2	0.7	39.5	0.4	272	170	0.4	0	2.1	6.2	7.7	0.7	4.9	2.2	17.9	5.7	331	136	0.2	0.1	12.9
15	9.1	10.4	1.7	7.4	0.9	36.5	3.1	294	161	0	0	8.4	6.9	8.8	0.5	5.2	1.9	27.0	4.5	356	126	0	0.1	11.2
20	6.6	8.2	0.8	5.0	1.1	29.7	3.1	291	164	0	0	8.4	3.5	7.9	0.9	3.2	1.5	36.0	6.2	405	140	0	0.1	15.0
25	2.9	9.5	1.4	2.7	0.6	50.6	5.1	303	173	0	0.1	11.8	4.4	7.3	0.7	4.7	1.6	30.5	6.5	431	150	0	0.1	15.7
	AS5												AS3											
1	[a]	6.0	0.8	5.4	3.7	78.8	[a]	325	104	0	0.1	8.1	[a]	7.5	1.1	4.2	2.2	146	[a]	362	122	0.9	0.4	34.0
2	[a]	7.1	1.0	5.6	4.8	56.6	[a]	365	112	0	0	1.2	[a]	11.0	3.8	5.8	1.4	113	[a]	391	115	0.5	0.2	21.6
3	6.8	7.1	1.0	5.2	3.3	24.9	0.2	318	110	0	0	2.1	3.1	7.1	0.3	3.8	0.7	17.7	0.3	328	88.7	0	0	1.4
4	5.4	6.8	1.6	5.6	2.1	22.1	0.3	324	120	0	0	2.2	4.4	6.3	0.4	4.9	0.7	18.5	0.3	334	87.4	0	0	1.4
5	6.4	7.0	1.5	4.5	2.3	23.9	0.2	338	120	0	0	2.2	2.8	6.7	0.4	3.6	0.6	19.2	0	340	90.0	0	0	1.4
6	11.1	12.3	5.3	5.4	3.0	32.8	0.3	328	119	0.2	0	2.3	2.8	6.4	0.2	3.9	0.6	20.6	0.2	341	87.5	0	0	1.5
7	6.7	6.2	1.3	4.2	2.2	25.5	0.1	345	120	0	0	1.7	3.1	6.7	0.3	4.7	0.7	24.6	0.4	364	91.6	0	0	2.3
8	5.3	7.3	1.4	3.9	2.1	25.2	0.2	352	120	0	0	1.9	3.0	7.1	1.0	4.6	0.7	25.1	0.5	380	99.4	0	0	3.1
9	4.5	10.4	3.8	3.4	1.5	25.7	1.8	345	125	0	0	5.9	4.0	7.6	1.3	5.4	0.7	25.9	0.3	373	96.4	0	0	2.6
10	7.2	7.0	1.2	4.1	3.0	24.1	0.7	351	130	0	0	3.4	2.8	7.8	1.1	4.1	0.8	26.7	0.1	372	95.5	0	0	2.3
15	6.3	10.9	1.1	5.4	2.0	26.1	3.5	403	128	0	0.1	9.7	4.8	9.2	1.0	5.6	1.6	21.6	3.7	368	105	0.1	0.1	10.8
20	9.3	9.4	0.4	6.5	2.2	27.0	4.5	410	125	0	0.1	11.8	5.2	8.5	0.4	6.1	1.6	13.4	3.1	173	91.8	0	0.1	7.5
25	8.1	8.7	0.8	6.1	1.6	19.5	5.9	433	136	0	0.1	14.0	7.6	7.5	0.3	6.6	2.2	13.3	0.7	133	78.3	0.1	0	1.6
	Ahla2												Ahla6											
1	2.0	3.9	2.2	2.0	1.5	69.8	0.5	358	104	0	0	3.3	3.9	5.5	1.8	4.1	1.2	32.3	0	660	122	0.1	0	4.5
2	1.8	4.2	2.3	0.8	0.8	72.5	0	387	109	0	0	3.5	3.6	5.9	2.0	2.2	1.0	28.7	0	649	122	0	0	3.3
3	1.6	3.8	1.8	1.0	0.6	61.4	0	381	110	0	0	3.5	4.5	6.9	2.2	2.6	1.3	24.7	1.0	662	124	0	0	7.0
5	1.5	4.1	1.9	0.7	0.4	38.1	0	372	106	0	0	3.1	4.2	5.5	1.5	2.8	1.0	18.1	0	690	120	0	0	3.5
7	2.0	4.0	2.0	1.2	0.4	11.7	0.3	365	105	0	0	3.7	4.0	5.4	1.6	2.9	0.9	15.7	0	731	121	0	0	4.2
10	2.4	3.1	1.3	1.7	0.6	9.8	0	335	98.4	0	0	3.1	4.1	5.2	1.4	3.0	1.4	15.2	0	699	124	0	0.1	4.1
15	2.5	2.9	1.4	1.7	0.5	4.9	0	288	109	0	0	2.7	6.6	21.1	7.8	5.0	2.3	19.0	0	675	125	0.2	0.1	3.9
25	3.2	3.6	1.2	1.2	0.5	1.9	0	397	93.4	0.1	0	2.5	4.9	6.5	1.1	4.4	2.9	25.0	0	645	119	0	0.1	3.6
	Ahla9																							
1	7.0	5.6	1.5	6.9	3.3	44.8	2.2	687	109	0.5	0	10.6												
2	11.6	10.1	2.5	5.0	5.4	64.1	0	1,038	156	0	0	3.8												
3	13.9	8.0	2.1	11.4	4.6	39.7	0	795	112	0.4	0	5.5												
5	16.2	10.0	1.7	12.2	5.8	51.3	0.1	959	122	0.2	0	4.6												

Table 5 continued

Depth (cm)	NaBD						NaOH						NaBD						NaOH					
	Mg	Si	Al	Ca	Mn	Fe	Mg	Si	Al	Ca	Mn	Fe	Mg	Si	Al	Ca	Mn	Fe	Mg	Si	Al	Ca	Mn	Fe
7	11.2	8.8	1.8	10.3	4.6	32.9	0	685	99.1	0	0	3.1												
10	10.2	9.1	1.6	9.2	3.4	36.6	0.9	939	130	0.4	0	8.3												
15	7.6	8.9	2.2	8.5	3.1	27.8	9.5	962	159	1.6	0.4	30.2												
25	7.1	9.8	2.1	9.3	4.3	36.9	7.8	938	160	1.3	0.3	28.6												

[a] Concentration of the element not determined

0 = concentration below detection limit or <0.05 μmol g^{-1} DW

Maximum concentration range for Mg, Si, Al, Ca, Mn, and Fe, respectively, of triplicate or duplicate samples: NaBD: <2.5, <14.5, <9.5, <4.4, <2.0, and <42.2; NaOH: <41.1, <93.1, <105, <20.4, <0.7, and <74.5

Table 6 Summary of statistically significant relationships between different P fractions, other elements in extracts, and sediment parameters

Dependent variable	Statistically significant relationship with
NaCl-iP	TP_{sed}, TC, TFe_{sed}, TMn_{sed}, TCa_{sed}, TS
NaBD-iP	TP_{sed}, TAl_{sed}, TN, TS, NRP, NaOH-iP, Res-P (NaBD-Mn)
NRP	TP_{sed}, NaBD-iP
NaOH-iP	TP_{sed}, TC, TCa_{sed}, TS, NaBD-iP (NaOH-Al, NaOH-Si)
HCl-iP	TP_{sed}, TC, TFe_{sed}, TCa_{sed}
Res-P	TP_{sed}, TC, TMn_{sed}, TAl_{sed}, TN, NaBD-iP
Total organic P	TP_{sed}, TFe_{sed}, TMn_{sed}, NRP
TP_{extr}	TP_{sed}, Total organic P, NaCl-iP, NaBD-iP, NaOH-iP, HCl-iP, Res-P

Sed (as a subscript) = content in the sediment

more or less uniform, suggesting that the quality and quantity of P in the deposited material were fairly constant over time. This could also indicate that the early diagenetic processes have had enough time to transform the deposited P into its final, buried form. However, the shallow water, the low SAR value, and the low clay content at Ahla2 (Fig. 3) suggest that this site is vulnerable to sediment transportation. Two contemporary peaks of oxide-bound P at Paila14 and AS5 indicate that eroded material had been transported as pulses from the upper reaches of the watershed, while the simultaneous increase in TP_{extr} at Ahla6 and Ahla9 indicates that sediment enrichment with P increased in the early 1980s. It can be concluded that the biogeochemical processes controlling vertical P distribution are partly masked in areas with high SAR. However, the chemical nature of deposited P determines whether it is permanently buried or further participates in the P cycle.

The vertical distribution of P fractions in these estuary sediments indicate that only a very small part of P was transformed in biogeochemical processes from one form into another (i.e., sink-switching; Froelich et al. 1982; Ruttenberg and Berner 1993), which has been found in several other studies in marine sediments (Ruttenberg and Berner 1993; Slomp et al. 1996b). A possible explanation for this is the high sedimentation rate in the estuaries: the examined material was relatively young and there may not have been enough time to complete reactions of P diagenesis. The fast sedimentation can also partly explain the decrease in TP_{extr} (in contrast to findings, e.g., by Ruttenberg and Berner 1993; Slomp et al. 1996a) with sediment depth (except at the two innermost sites): new material accumulates to the surface, while the biogeochemical processes are still transforming the subsurface material.

Immobile P

Typically, immobile P dominated (33–76%) at the sites with lowest SAR. Its concentration did not change appreciably with sediment depth. However, it became the dominating P form in the deep layers, where the reactive P was diminished (see also Coelho et al. 2004).

The portion of NaOH-iP of TP_{extr} in general varied only slightly, indicating stability of this fraction in natural conditions (Fig. 2a, b). It represents P that is strongly bound to oxides of Al and Fe through the formation of binuclear or bidentate inner-sphere complexes (Hingston et al. 1967). NaOH may also extract P from organometallic complexes (Schnitzer 1969; Gerke and Hermann 1992; Lopez 2004). P bound to oxide surfaces by monodentate binding is replaceable with competing anions and mobile in natural conditions (e.g., with increase in pH) (e.g., White 1980). However, we suppose that a small part of the oxide-bound P may have already been lost in the preceding (NaBD) extraction due to the use of sodium bicarbonate ($NaHCO_3$) as buffer and pH 7 (Olsen et al. 1954). In a separate test made solely with $NaHCO_3$, 14% of P extracted with NaBD was released at this step from subsurface sediment collected from oxic area in the GoF. Quantitatively, NaOH-iP was lowest at the outermost site (AS3). Similarly, Coelho et al. (2004) reported a decreasing trend in NaOH-iP towards the mouth of the Mondego estuary in Portugal. In our work, the positive correlation and statistically significant dependence between NaOH-iP and NaOH-Al (Table 6) (see also Lopez 2004) can be explained by the partial dissolution of Al from poorly crystallized oxides through formation of aluminate anions (see Lindsay 1979). Thus, the high NaOH-Al content in the inner estuary of Paila Bay (Table 5) may indicate the abundance of Al oxides able to retain P. Our conclusion is supported by findings of Lebo (1991) in the Delaware Estuary (USA): about 23% of P in suspended particles was associated with Al oxides, while 27% was associated with Fe oxides. On the other hand, Forsgren and Jansson (1993) concluded that in the River Öre Estuary (BS) Al was less important than Fe in P binding. Although NaOH-extractable Fe was clearly lower than NaBD-extractable Fe (Table 5), its presence suggests that the NaBD did not remove Fe efficiently. However, in our previous study, NaBD extracted 28% of total Fe from calcareous river sediment, while NaOH extracted only 1% of it (Lukkari et al. 2007b). Similarly to Al, NaOH-extractable Fe may have partly originated from oxide surfaces. Nevertheless, NaOH extracts organic matter and part of both Al and Fe may have originated in humic complexes (Schnitzer 1969). The abundance of Si in NaOH in Ahla Bay (Table 5) suggests that this estuary was rich in biogenic Si, and P binding may be affected through competition of sorption sites on oxide surfaces (Hingston et al. 1967; Hartikainen et al. 1996). On the other hand, NaOH may also release Si from silicate structures (e.g., Jones and Dreher 1996).

As expected, the apatite-P fraction (HCl-iP) was fairly stable in the profiles (Fig. 2a, b) (see also Salomons and Gerritse 1981). The accumulation of this P form was highest at the shallowest site (Ahla2) in agreement with findings of Forsgren and Jansson (1993) and Lopez (2004). Material at Ahla2 was coarsest in texture (Fig. 3) probably because the fine material had been transported farther, leaving behind the high-density apatite mineral. Berner and Rao (1994) found in the Amazon River Estuary that Ca-P and Fe-P accumulated in different areas. In our study, the negative correlation between HCl-iP and NaOH-iP (and NaOH-Al) may indicate that the primary and secondary P differed in their preferential accumulation areas. However, in this study, apatite-P includes both detrital and authigenic apatite-P, because the authigenic apatite-P, a reactive P fraction, which acts as sink for P (Ruttenberg 1992), is not separated in the method by Jensen and Thamdrup (1993). HCl-iP may also contain other inorganic P phases (Ruttenberg 1992). Virtasalo et al. (2005) examined surface sediments in the AS using the SEDEX-method (Ruttenberg 1992; modified by Anderson and Delaney 2000), and found that, on average, authigenic apatite-P formed 8–12% of TP_{extr}, while detrital apatite-P formed 27–35% of TP_{extr}. The portion of detrital apatite-P is probably higher in sediments of the estuaries than the AS.

The Res-P fraction, i.e., the refractory organic P, represents P incorporated in the refractory humic material, though it is assumed to contain some inorganic P as well (Williams et al. 1967, 1980; Ruttenberg 1992; Lopez 2004), possibly apatite-P and P occluded in oxide structures (e.g., Chang and Jackson 1957; Psenner et al. 1984). Res-P formed a considerable portion of TP_{extr} and did not show marked vertical or spatial variation (Fig. 2a, b). Forsgren and Jansson (1993) reported almost constant distribution of residual P in the Öre River Estuary.

Reactive P

About half of the TP_{extr} consisted of P in fractions considered reactive. Sediment reactive P includes forms that, under favourable conditions, are transformed in various biogeochemical reactions into P potentially available for algae and bacteria (i.e., dissolved PO_4–P or P in small molecules). As an example, NaBD-iP can be released from reducing Fe compounds, and part of the organic P in the NRP fraction can be degraded into inorganic P. The reactive P dominated (25–68%) at sites with highest SAR (Paila14, AS5, and Ahla9). At other sites, it generally decreased with sediment depth, indicating reduction-induced P release from Fe compounds or degradation of organic P (Krom and Berner 1981; Berner and Rao 1994).

Even though soluble P (NaCl-iP) comprised only a small portion of TP_{extr} in all samples (Fig. 2a, b), it is important because it can diffuse to the water column and it is directly available for bacteria and algae (Van Eck 1982). This fraction was highest at Ahla9, where the content of reactive P and outward incubation-derived PO_4–P flux were highest.

The generally decreasing trend of reductant soluble P and Fe with sediment depth (and redox-potential) (Figs. 2a, b, 4; Table 5) can be attributed to reduction of Fe^{3+} (and Mn^{4+}) in subsurface layers and consequent liberation of P, as well as to entrapment of diffused PO_4–P onto oxidized Fe compounds in the surface sediment (e.g., Mortimer 1942; Krom and Berner 1980; Salomons and Gerritse 1981; Balzer 1986; Sundby et al. 1992; Anschutz et al. 1998). Nevertheless, chemically reducible Fe and P bound to it were also found in the deep sediment layers, in agreement with earlier reports (Balzer 1986; Lovley and Phillips 1986; Jensen and Thamdrup 1993; Berner et al. 1993; Ruttenberg and Berner 1993; Slomp et al. 1996b; Hyacinthe and Van Cappellen 2004). There are several possible explanations for this. (1) It is likely that NaBD extraction is efficient enough to liberate Fe from compounds not reducible in natural conditions and to dissolve crystalline Fe oxides (e.g., Bauwin and Tyner 1957; Mehra and Jackson 1960; Williams et al. 1971; Ruttenberg 1992; Jensen and Thamdrup 1993). (2) Adsorbed ligands (e.g., humic compounds) and the formation of organometallic compounds may make the Fe compounds more resistant to microbial reduction (Schnitzer 1969; Suzumura and Kamatani 1995). As suggested by Hyacinthe and Van Cappellen (2004), an abundance of Fe^{2+} on oxide surfaces in reduced sediment hinders the microbial reduction of Fe^{3+} in oxides. (3) As proposed by Lovley and Phillips (1986), the presence of oxalate-extractable Fe^{3+} compounds at up to 20-cm depth in estuary sediment could be explained by the occurrence of mixed Fe^{3+}–Fe^{2+} compounds resistant to reduction. (4) NaBD may have extracted some P from short-range order Al oxides containing Fe oxides as impurities (Williams et al. 1971) or some P may have been desorbed from Al oxides by the bicarbonate used in the previous step (Olsen et al. 1954; Kamprath and Watson 1980). (5) The dissolution of Fe oxides in dithionite may have released occluded P (Chang and Jackson 1957; Mehra and Jackson 1960; Williams et al. 1971; Agbenin 2003). Hyacinthe et al. (2006) concluded that chemical reduction of sediment Fe^{3+} overestimates that reduced by microorganisms because of physical occlusion.

In our samples, the lack of statistically significant relationship between reductant soluble P and Fe indicates that not all Fe dissolved in the second step is active in P binding. The Fe:P ratio in the reductant has sometimes been used to assess the P retention ability (e.g., Jensen and Thamdrup 1993; Coelho et al. 2004). In our estuary sediments, however, this ratio was highly variable (1.1–9.2 at 1-cm depth) and was not consistent with the corresponding incubation-derived P flux measurements. Nevertheless, the ratio was lowest at the most reduced sites (Ahla6 and Ahla9).

In addition to vertical variation, the reductant soluble P also showed the most pronounced spatial variation, and this seemed to be related to SAR (Table 4) or to the quality of deposited material. SAR was lower in Ahla Bay than in Paila Bay, but reductant soluble P was higher (except at Ahla2). It is unlikely that the sediment at Ahla Bay trapped P more efficiently, because the outward incubation-derived PO_4-P flux was highest at Ahla9 and Ahla6 was the most reduced site (Table 2; Fig. 4). Probably, then the material deposited in Ahla Bay was originally richer in Fe-P not sensitive to natural reduction (e.g., in occluded P; Chang and Jackson 1957; Mehra and Jackson 1960; Williams et al. 1971; Agbenin 2003; Hyacinthe et al. 2006) or the conditions in the sediment favoured more incomplete reduction of Fe compounds and burial of P (e.g., because of association with humic compounds; Schnitzer 1969; Suzumura and Kamatani 1995).

The more or less stable vertical distribution of NRP indicates that most of it is resistant or slowly degradable in the estuary sediment and will be buried. Recently, pyrophosphate, polyphosphate, and orthophosphate mono- and diesters were identified in the NRP fraction (Ahlgren et al. 2005; Reitzel et al. 2006). Ahlgren et al. (2005) estimated that half-lives of biogenic P compounds ranged from 13 to 23 years in lake sediments and proposed that their degradation would be faster in anoxic brackish water sediment than in lake sediment. Retention of organic (biogenic) P compounds onto oxide surfaces with a binding mechanism similar to that of PO_4-P retards their degradation (e.g., Suzumura and Kamatani 1995; Celi et al. 1999). In our estuary sediments, the high SAR (and perhaps the incomplete Fe reduction) magnified the impact of this phenomenon, favouring the burial of NRP. The abundance of the NRP fraction at the outermost site AS3 may be attributable to the transport of humic matter from the inner estuary towards the open sea. Although increasing salinity enhances the aggregation and deposition of humic matter and Fe-P complexes in an estuary (e.g., Sholkovitz 1976; Forsgren and Jansson 1992, 1993), this pattern is not relevant among our sites in Paila Bay, because the salinity did not change much. However, the composition of NRP probably changes along the estuary (from compounds of terrestrial origin to those of more aquatic origin; e.g., Martens and Goldhaber 1978; Stepanauskas et al. 2002), and this affects the degradability of NRP. Ruttenberg and Goñi (1997) assessed the origin of sediment OM on the basis of total organic C:P and C:N, assuming that these ratios would be higher in terrestrial than in marine phytodetritus. If TC and TN in our sediments can be considered organic (which is supported by their positive correlation with NRP), it is likely that the two innermost sites in Ahla Bay, where C:P and C:N ratios were high, were richer in OM of terrestrial origin than the outermost sites in Paila Bay, where ratios were lower. This is in agreement with the high TOC load to Ahla Bay.

Results of the PCA were in agreement with the theoretical basis of the method and our previous conclusions on the relations between various P fractions and sediment variables. Sediment C and N followed the labile organic P fraction (NRP), while Ca followed apatite-P. Parameters dependent on the redox conditions were grouped. However, sediment Fe was partly distributed to the same factor with Al and metal oxide-bound P, possibly indicating its presence in compounds not sensitive to reduction. The dissolved P was separated from the solid fractions, while several sediment parameters seemed to affect the grouping of the residual P of undefined composition.

Impact of sediment properties on dissolved P and N species

The trend in P accumulation and the sediment characteristics were reflected in the chemistry of the near-bottom water and pore water. Sediment TP_{extr} and PO_4–P in the near-bottom water were highest at Ahla9 and Ahla6 (Table 2; Fig. 2a, b). The pronounced release of PO_4–P from sediment at Ahla9 agreed with the finding of high concentration and steep gradient of pore water PO_4–P at this site. In fact, at Ahla9, which was high in sediment TN, the high near-bottom water NH_4–N and steep pore water NH_4–N profile indicate intense degradation of OM and consequent release of nutrients (e.g., Martens and Goldhaber 1978; Krom and Berner 1981; Kamp-Nielsen 1992). The second highest bottom water PO_4–P was found at Ahla6, where conditions at the sediment-water interface were most reducing (Fig. 4). Sulfur has been reported to affect sediment P release via Fe chemistry (e.g., Berner 1970; Jørgensen 1977; Martens and Goldhaber 1978; Krom and Berner 1980, 1981; Caraco et al. 1989; Anschutz et al. 1998): precipitation of Fe-sulfides lowers the ability of Fe to diffuse to the oxidized zone and participate in P binding. Black laminas at 2–3 cm depth at AS5 and Paila14 can be taken as indications of this reaction. In fact, at both sites, P bound to reducible Fe was low at this depth, while the peak values immediately above indicate entrapment of P that had diffused upwards (Fig. 2a). Furthermore, in agreement with this, concentration of pore water PO_4–P increases below 3-cm depth, especially at Paila14 (Fig. 2a). Similarly, high TS at the organic rich Ahla9 site may be related to microbiological sulfate reduction and Fe-sulfide formation and, as a consequence, to pronounced P release. This is supported by the elevated pH (Martens and Goldhaber 1978; Caraco et al. 1989) at this site (Fig. 4).

The lower incubation-derived PO_4–P flux and near-bottom water PO_4–P in Paila Bay can be attributed to the high Fe and Al concentrations (Table 3) in material transported from the drainage area of the River Paimionjoki. The material eroded from the clayey soils typical of southern Finland is rich in poorly crystallized Al and Fe oxides which are active in P retention (Hartikainen 1979; Uusitalo 2004; Peltovuori 2006). Even though the total metal concentrations in sediment cannot be considered ecologically relevant, they may be indicative of forms active in P binding. It is noteworthy that sediment Al was about three-fold sediment Fe and generally higher in Paila Bay. This gives reason to suppose that Al compounds contribute to P binding in these estuaries. The finding that NaOH dissolved more Al in Paila Bay than in Ahla Bay supports this hypothesis. On the basis of Al chemistry, Al in this extract can be considered to have originated in reactive oxides, even though the P fractionation procedure is not specific for Al. Because the sorption ability of Al oxides is not redox dependent (Psenner et al. 1984), the role of these oxides as sorbents for P is emphasized in areas suffering from hypoxia. Fe oxides, on the other hand, although equally effective in P binding, react to O_2 depletion by releasing sorbed P (e.g., Mortimer 1941, 1942). An example of this can be seen in the sole anoxic site, AS5 (in Paila Bay). A small negative incubation-derived PO_4–P flux (Table 2) co-occurring with low pore water PO_4–P and high near-bottom water NO_3–N (Fig. 2a) suggests that the O_2 conditions may have recently improved there, enhancing binding of PO_4–P to re-oxidized Fe compounds. The gradients of pore water Fe and Mn support this conclusion.

Burial and potential for release of sediment P

The immobile P forms (NaOH-iP, HCl-iP, and Res-P) are considered to represent P that is permanently removed from the nutrient cycle and the reactive P forms (NaCl-iP, NaBD-iP, and NRP) represent P that may become available for bacteria and algae. This rough division did not unambiguously represent the situation in our estuary sediments. The reactive fraction, which is assumed to decrease with sediment depth, was also abundant in deeper layers, indicating that part of the reactive P also becomes permanently buried. In our case, therefore, the amount of reactive P in deeper layers was taken into account in order to obtain more reliable estimates of the part of deposited P that becomes buried. The reactive P found in each sediment profile at the depths of ^{137}Cs-maxima (i.e., year 1986) was considered as a "site specific background value" (see also Hyacinthe et al. 2006) for buried reactive P and was added to the immobile P in the surface sediment in calculating the burial flux for deposited P. Thus, the remainder of the reactive P in the surface sediment represents "potentially mobile P", vulnerable to release from the sediment in biogeochemical processes. In this approach, we assume that the quantity and quality of the deposited material at each site remain more or less constant. However, it should be kept in mind that these factors vary and are affected by environmental conditions at the sediment-water interface (e.g., O_2 conditions, reactive sorption components for P, and OM and bioturbation). Furthermore, if we assume that all reactive P lost was released from the sediment to water and that the sedimentation rate was constant, we can evaluate the amount of reactive P lost between 1986 (i.e., the year with ^{137}Cs maxima) and the sampling year, and roughly estimate a long-term average of annual P release. It is likely that in our estuary sediments the assumptions presented above are not entirely fulfilled. For example, sedimentation rate depends on annual precipitation, water flows, and transportation of particulate matter. However, the risk for release of sediment P is highest in areas rich in "potentially mobile P", especially in the surface sediment. Thus, in our study area, under favourable conditions, sites Paila14 and AS5 would show the highest effluxes of sediment P (Table 4).

In general, the burial flux (28–209 mmol m^{-2} y^{-1}) and the burial efficiency (52–90%) of P (Table 4) were high in these estuaries. Relatively high burial fluxes and efficiencies for P have also been reported in other estuaries and coastal areas. Kamp-Nielsen (1992), using sediment traps in the brackish Roskilde Fjord, Denmark, recorded P sedimentation of 226–1,679 mmol P m^{-2} y^{-1} and concluded that a major part of it was buried. In the shallow Aarhus Bay, Jensen et al. (1995) recorded sedimentation between 51 and 63 mmol P m^{-2} y^{-1} with burial flux of 18 mmol P m^{-2} y^{-1} and a sediment P release of 34 mmol P m^{-2} y^{-1}. Sundby et al. (1992) evaluated that about half of particulate P flux in the Laurentian Trough (the Gulf of St. Lawrence) was returned back to water column, while Anschutz et al. (1998) evaluated that 20–30% of P in the surface of several continental margin sediments was remobilized. Filippelli (2001) reported that the common burial rates of 5–80 mmol m^{-2} y^{-1} for continental margin sediments were greatly exceeded in the Saanich Inlet (British Columbia), where the long-term burial rates of reactive P ranged from 100 to 600 mmol m^{-2} y^{-1}. It is likely that bioturbation had influenced P burial at most of our sites. Bioturbation can create a complex three-dimensional structure in the sediment and enhance

P binding via the formation of Fe(III) oxyhydroxides by oxidizing the sediment, enhance P burial by mixing P-rich particulates into deeper sediment layers, or enhance mixing of high PO_4–P pore water from deep sediment layers into the overlaying water column (e.g., Aller 1988; Kristensen 1988; Andersen and Jensen 1991; Sundby et al. 1992; Lewandowski and Hupfer 2005).

Chemical characterization of sediment P indicates that these two estuaries mainly act as traps for P-containing material transported from the drainage area. The high SAR controls the burial of P (see also Ingall and Jahnke 1994) and retards the release of P from the reactive forms of the deposited P. In addition, it seems that the preservation and burial of Fe oxides may act as an important sink for P, as previously suggested by Lovley and Phillips (1986), Berner et al. (1993), Slomp et al. (1996b), Filippelli (2001), and Hyacinthe and Van Cappellen (2004). Despite the extensive burial, incubation-derived PO_4–P flux measurements indicated some release of P at most of the sites. This flux differed from the long-term P efflux calculated on the basis of P fractionation results. However, the flux measurement of dissolved PO_4–P reflects a temporary situation, while P efflux, calculated on the basis of the chemical character of sediment P, is a consequence of long-term biogeochemical processes. Furthermore, the patchiness of the small sedimentary basins in the estuaries creates variable conditions that may result in P release at one site and burial at a neighbouring one.

Conclusions

Large amounts of P were accumulated in sediments of the shallow, clay and organic rich estuaries of this study. P fractionation revealed that about half of the sediment P was in forms prone to release P to the water column under anoxic conditions or as a result of microbiological degradation of organic compounds and other diagenetic processes. This reactive P fraction was slightly higher at sites with the highest sedimentation rates and decreased with sediment depth. A similar pattern was found for Fe-bound P (the dominant reactive P form), which also showed high vertical and spatial variation. Labile organic P was relatively most abundant at the outermost sampling site. Concentration of the pore water P was small compared with other sediment P forms. Immobile P dominated at sites with lowest sedimentation rate and all immobile P forms were more or less constant in the sediment depth profile. Apatite-P tended to dominate where the portion of reactive P decreased, while residual P showed little spatial variation. The amount of P bound to Al oxides and other metal compounds that were not reduced chemically was relatively most abundant at the innermost sites of Paila Bay rich in eroded material.

The studied estuaries differed in sediment properties, which were reflected in their P reserves. Properties associated with reactive P forms were OM and reducible metal compounds, while those associated with immobile P were Ca and Al. Furthermore, the nutrient chemistry of the near-bottom water and pore water reflected the accumulation of P and the sediment characteristics. At the time of sampling, most of the sites showed outward incubation-derived P flux. Our results nevertheless indicate that, in the long term, these estuaries have mainly acted as sinks for deposited P, restricting transportation of P to the open GoF and AS and partly alleviating the eutrophication process. Removal of deposited P from the nutrient cycling was most efficient at innermost estuary. However, the high sedimentation rate controlled P accumulation and burial and appeared to mask the biogeochemical processes influencing the vertical distribution of P.

The P fractionation procedure distinguishing the major inorganic and organic P forms is a useful tool for investigating the chemical character of P in sediments. Overall, our results are in accordance with earlier reported sediment parameters and environmental variables controlling P sorption. When evaluating burial flux of P, vertical distribution of both immobile P and reactive P forms should be considered because the burial of P depends on several site-specific properties related, among other things, to sedimentation. Sequential extraction nevertheless is a rough method involving some uncertainties, and the results need to be interpreted carefully. In estuary sediments, for example, differences in sedimentation, erosion of the sediment surface, and vertical and spatial heterogeneity in the sediments should be taken into account.

Acknowledgments Financial support was received from the Ministry of the Environment, the Kone Foundation, the Finnish Institute of Marine Research, and the Maj and Tor Nessling Foundation. We warmly thank the technicians from the laboratory of the Finnish Institute of Marine Research for assistance in the P fractionation; the laboratory for Environmental Research, University of Jyväskylä, for the metal determinations; Aarno Kotilainen, Henry Vallius, Jyrki Hämäläinen, Kimmo Alvi, and Boris Winterhalter from the Geological Survey of Finland for providing sediment descriptions and photographs and for echo sounding during cruises of r/v Aranda; Kalervo Mäkelä and Hannu Haahti from FIMR for the sediment pore water data and the nutrient flux measurements; the personnel of r/v Aranda, r/v Muikku, and r/v Aurelia for assistance during cruises; and Ville Hallikainen, Risto Häkkinen, Jaakko Heinonen, and Juha Hyvönen from the Finnish Forest Research Institute for advice on the statistical analysis, especially in regard to the mixed model. This study was part of a project within the SEGUE consortium (Searching for protection tools for the eutrophied Gulf of Finland—Integrated use of research and modelling tools) carried out in collaboration between the Finnish Institute of Marine Research, the Finnish Environment Institute, and the University of Helsinki. SEGUE is part of the Baltic Sea Research Programme (BIREME) organized by the Academy of Finland.

References

Agbenin JO (2003) Extractable iron and aluminium effects on phosphate sorption in a savanna alfisol. Soil Sci Soc Am J 67:589–595

Ahlgren J, Tranvik L, Gogoll A, Waldebäck M, Markides K, Rydin E (2005) Sediment depth attenuation of biogenic phosphorus compounds measured by ^{31}P NMR. Environ Sci Technol 39:867–872. doi:10.1021/es049590h

Aller RC (1988) Benthic fauna and biogeochemical processes in marine sediments: the role of burrow structures. In: Blackburn TH, Sørensen J (eds) Nitrogen cycling in coastal marine environments. Wiley, Chichester, pp 301–338

Andersen FØ, Jensen HS (1991) The influence of chironomids on decomposition of organic matter and nutrient exchange in a lake sediment. Verh Int Ver Limnol 24:3051–3055

Anderson LD, Delaney ML (2000) Sequential extraction and analysis of phosphorus in marine sediments: streamlining of the SEDEX procedure. Limnol Oceanogr 45(2):509–515

Anderson LD, Delaney ML, Faul KL (2001) Carbon to phosphorus ratios in sediments: Implications for nutrient cycling. Global Biogeochem Cycles 15(1):65–79. doi:10.1029/2000GB001270

Anschutz P, Zhong S, Sundby B, Mucci A, Gobeil C (1998) Burial efficiency of phosphorus and the geochemistry of iron in continental margin sediments. Limnol Oceanogr 43(1):53–64

Balzer W (1986) Forms of phosphorus and its accumulation in coastal sediments of Kieler Bucht. Ophelia 26:19–35

Bauwin GR, Tyner EH (1957) The nature of reductant-soluble phosphorus in soils and soil concretions. Soil Sci Soc Am Proc 21:250–257

Bender M, Martin W, Hess J, Sayles F, Ball L, Lambert C (1987) A whole-core squeezer for interfacial pore-water sampling. Limnol Oceanogr 32(6):1214–1225

Berner RA (1970) Sedimentary pyrite formation. Am J Sci 268:1–23

Berner RA, Rao J-L (1994) Phosphorus in sediments of the Amazon River and estuary: implications for the global flux of phosphorus to the sea. Geochim Cosmochim Acta 58(10):2333–2339. doi:10.1016/0016-7037(94)90014-0

Berner RA, Ruttenberg KC, Ingall ED, Rao J-L (1993) The nature of phosphorus burial in modern marine sediments. In: Wollast R, Mackenzie FT, Chou L (eds) Interactions of C, N, P and S biogeochemical cycles and global change. NATO ASI series, 14. Springer, Berlin, pp 365–378

Caraco NF, Cole JJ, Likens GE (1989) Evidence for sulphate-controlled phosphorus release from sediments of aquatic systems. Nature 341:316–318. doi:10.1038/341316a0

Celi L, Lamacchia S, Marsan FA, Barberis E (1999) Interaction of inositol hexaphosphate on clays: adsorption and charging phenomena. Soil Sci 164(8):574–585. doi:10.1097/00010694-199908000-00005

Chang SC, Jackson ML (1957) Fractionation of soil phosphorus. Soil Sci 84:133–144. doi:10.1097/00010694-195708000-00005

Coelho JP, Flindt MR, Jensen HS, Lillebø AI, Pardal MA (2004) Phosphorus speciation and availability in intertidal sediments of a temperate estuary: relation to eutrophication and annual P fluxes. Estuar Coast Shelf Sci 61:583–590

Delaney ML (1998) Phosphorus accumulation in marine sediments and the oceanic phosphorus cycle. Global Biogeochem Cycles 12(4):563–572. doi:10.1029/98GB02263

Einsele W (1936) Über die Beziehungen des Eisenkreislaufs zum Phophatkreislauf im eutrophen See. Arch Hydrobiol 29:664–686

Emeis K-C, Struck U, Leipe T, Pollehne F, Kunzendorf H, Christiansen C (2000) Changes in the C, N, P Burial rates in some Baltic Sea sediments over the last 150 years—relevance to P regeneration rates and the phosphorus cycle. Mar Geol 167:43–59. doi:10.1016/S0025-3227(00)00015-3

Filippelli GM (2001) Carbon and phosphorus cycling in anoxic sediments of the Saanich Inlet, British Columbia. Mar Geol 174:307–321. doi:10.1016/S0025-3227(00)00157-2

Forsgren G, Jansson M (1992) The turnover of river-transported iron, phosphorus and organic carbon in the Öre estuary, northern Sweden. Hydrobiologia 235/236:585–596. doi:10.1007/BF00026246

Forsgren G, Jansson M (1993) Sedimentation of phosphorus in limnetic and estuarine environments in the River Öre system, northern Sweden. Hydrobiologia 253:233–248. doi:10.1007/BF00050745

Frankowski L, Bolalek J, Szostek A (2002) Phosphorus in bottom sediment of Pomeranian Bay (Southern Baltic-Poland). Estuar Coast Shelf Sci 54:1027–1038. doi:10.1006/ecss.2001.0874

Froelich PN (1988) Kinetic control of dissolved phosphate in natural rivers and estuaries: a primer on the phosphate buffer mechanism. Limnol Oceanogr 33(4):649–668

Froelich PN, Bender ML, Luedtke NA, Heath GR, DeVries T (1982) The marine phosphorus cycle. Am J Sci 282:474–511

Gerke J, Hermann R (1992) Adsorption of orthophosphate to humic-Fe-complexes and to amorphous Fe-oxide. Z Pflanzenernähr Bodenk 155:233–236. doi:10.1002/jpln.19921550313

Grasshoff K (1983) Determination of oxygen. In: Grasshoff K, Ehrhardt M, Kremling K (eds) Methods of seawater analysis, 2nd edn. Verlag Chemie Gmbh, Weinheim, pp 61–72

Hansen HP, Koroleff F (1999) Determination of nutrients. In: Grasshoff K, Kremling K, Ehrhardt M (eds) Methods of seawater analysis, 3rd edn. Verlag Chemie Gmbh, Weinheim, pp 159–228

Hartikainen H (1979) Phosphorus and its reactions in terrestrial soils and lake sediments. J Sci Agric Soc Finl 51(8): 537–624

Hartikainen H, Pitkänen M, Kairesalo T, Tuominen L (1996) Co-occurrence and potential chemical competition of phosphorus and silicon in lake sediment. Water Res 30(10):2472–2478. doi:10.1016/0043-1354(96)00139-X

HELCOM (1998) The Third Baltic Sea pollution load compilation (PLC 3). Baltic Sea environment proceedings, No. 70, Karisto Oy, Hämeenlinna, p 133

HELCOM (2003) The Baltic marine environment 1999–2002. Baltic Sea environment proceedings, No. 87. Erweko Painotuote Oy, Helsinki, p 47

Hingston FJ, Atkinson RJ, Posner AM, Quirk JP (1967) Specific adsorption of anions. Nature 215:1459–1461. doi:10.1038/2151459a0

Hyacinthe C, Van Cappellen P (2004) An authigenic iron phosphate phase in estuarine sediments: composition, formation and chemical reactivity. Mar Chem 91:227–251. doi:10.1016/j.marchem.2004.04.006

Hyacinthe C, Bonneville S, Van Cappellen P (2006) Reactive iron(III) in sediments: chemical versus microbial extractions. Geochim Cosmochim Acta 70:4166–4180. doi:10.1016/j.gca.2006.05.018

Ingall E, Jahnke R (1994) Evidence for enhanced phosphorus regeneration from marine sediments overlain by oxygen depleted waters. Geochim Cosmochim Acta 58(11):2571–2575. doi:10.1016/0016-7037(94)90033-7

Jensen HS, Thamdrup B (1993) Iron bound phosphorus in marine sediments as measured by bicarbonate-dithionite extraction. Hydrobiologia 253:47–59. doi:10.1007/BF00050721

Jensen HS, Mortensen PB, Andersen FØ, Rasmussen E, Jensen A (1995) Phosphorus cycling in a coastal marine sediment, Aarhus Bay, Denmark. Limnol Oceanogr 40(5):908–917

Jones RL, Dreher GB (1996) Silicon. In: Sparks DL, Bartels JM (eds) Methods of soil analysis. Part 3. Chemical methods. Soil Science Society of America book series, No. 5. Soil Science Society of America, Madison, WI, pp 627–637

Jørgensen BB (1977) The sulfur cycle of a coastal marine sediment (Limfjorden, Denmark). Limnol Oceanogr 22(5): 814–832

Kamp-Nielsen L (1992) Benthic-pelagic coupling of nutrient metabolism along an estuarine eutrophication gradient. Hydrobiologia 235/236:457–470. doi:10.1007/BF00026234

Kamprath EJ, Watson ME (1980) Conventional soil and tissue tests for assessing the phosphorus status of soils. In: Kasawneh FE, Sample EC, Kamprath EJ (eds) The role of phosphorus in agriculture. ASA-CSSA-SSSA, Madison, WI, pp 433–469

Kangas P, Bäck S, Kauppila P (eds) (2003) Ehdotuksia Euroopan yhteisön vesipolitiikan puitedirektiivin (2000/60/EY) mukaiseksi rannikkovesien tyypittelyksi Suomessa. Suggestions for a Typology of Coastal Waters for the Finnish Coast According to the European Union Water Framework Directive (2000/60/EY). Suomen Ympäristökeskuksen moniste, 284. Edita Oy, Helsinki, p 51. In Finnish

Kankaanpää H, Vallius H, Sandman O, Niemistö L (1997) Determination of recent sedimentation in the Gulf of Finland using 137-Cs. Oceanol Acta 20(6):823–836

Koroleff F (1983) Determination of phosphorus. In: Grasshoff K, Ehrhardt M, Kremling K (eds) Methods of seawater analysis, 2nd edn. Verlag Chemie Gmbh, Weinheim, pp 125–142

Kristensen E (1988) Benthic fauna and biogeochemical processes in marine sediments: microbial activities and fluxes. In: Blackburn TH, Sørensen J (eds) Nitrogen cycling in coastal marine environment. Wiley, Chichester, pp 275–299

Krom MD, Berner RA (1980) Adsorption of phosphate in anoxic marine sediments. Limnol Oceanogr 25(5):797–806

Krom MD, Berner RA (1981) The diagenesis of phosphorus in a nearshore marine sediment. Geochim Cosmochim Acta 45:207–216. doi:10.1016/0016-7037(81)90164-2

Kyzyurov V, Mikheev Y, Niemistö L, Winterhalter B, Häsänen E, Ilus E (1994) Shipboard determination of deposition rates of recent sediments based on Chernobyl derived Cesium-137. Baltica 8:64–67

Lebo ME (1991) Particle-bound phosphorus along an urbanized coastal plain estuary. Mar Chem 34:225–246. doi:10.1016/0304-4203(91)90005-H

Leivuori M (2000) Distribution and accumulation of metals in sediments of the northern Baltic Sea. Finnish Institute of Marine Research—Contributions, No. 2. Dissertation, University of Helsinki

Lewandowski J, Hupfer M (2005) Effect of macrozoobenthos on two-dimensional small-scale heterogeneity of pore water phosphorus concentrations in lake sediments: a laboratory study. Limnol Oceanogr 50(4):1106–1118

Lindsay WL (1979) Chemical equilibria in soils. Wiley, New York, p 449

Lopez P (2004) Spatial distribution of sedimentary P pools in a Mediterranean coastal lagoon ‘Albufera d’es Grau’ (Minorca Island, Spain). Mar Geol 203:161–176. doi:10.1016/S0025-3227(03)00333-5

Loring DH, Rantala RTT (1992) Manual for the geochemical analyses of marine sediments and suspended particulate matter. Earth Sci Rev 32:235–283. doi:10.1016/0012-8252(92)90001-A

Louchouarn P, Lucotte M, Duchemin E, de Vernal A (1997) Early diagenetic processes in recent sediments of the Gulf of St-Lawrence: phosphorus, carbon and iron burial rates. Mar Geol 139:181–200. doi:10.1016/S0025-3227(96)00110-7

Lovley DR, Phillips EJP (1986) Availability of ferric iron for microbial reduction in bottom sediments of the freshwater tidal Potomac River. Appl Environ Microbiol 52(4): 751–757

Lukkari K, Leivuori M, Hartikainen H (2007b) Fractionation of sediment phosphorus revisited: II Changes in phosphorus fractions during sampling and storing in the presence or absence of oxygen. Limnol Oceanogr Methods 5:445–456

Lukkari K, Hartikanen H, Leivuori M (2007a) Fractionation of sediment phosphorus revisited: I Fractionation steps and their biogeochemical basis. Limnol Oceanogr Methods 5:433–444

Maher WA, DeVries M (1994) The release of phosphorus from oxygenated estuarine sediments. Chem Geol 112:91–104. doi:10.1016/0009-2541(94)90106-6

Mäkelä K, Tuominen L (2003) Pore water nutrient profiles and dynamics in soft bottoms of the northern Baltic Sea. Hydrobiologia 492:43–53. doi:10.1023/A:1024809710854

Martens CS, Goldhaber MB (1978) Early diagenesis in transitional sedimentary environments of the White Oak River Estuary, North Carolina. Limnol Oceanogr 23(3):428–441

Mattila J, Kankaanpää H, Ilus E (2006) Estimation of recent sediment accumulation rates in the Baltic Sea using artificial radionuclides ^{137}Cs and ^{239,240}Pu as time markers. Boreal Environ Res 11:95–107

Mehra OP, Jackson ML (1960) Iron oxide removal from soils and clays by a dithionite-citrate system buffered with sodium bicarbonate. Clays Clay Miner 7:317–327. doi:10.1346/CCMN.1958.0070122

Mortimer CH (1941) The exchange of dissolved substances between mud and water in lakes, I. J Ecol 29:280–329. doi:10.2307/2256395

Mortimer CH (1942) The exchange of dissolved substances between mud and water in lakes, II. J Ecol 30:147–201. doi:10.2307/2256691

Olsen SR, Cole VR, Watanabe, FS, Dean LA (1954) Estimating available phosphorus by extraction with sodium bicarbonate. United States Department of Agriculture, Circular No. 939

Peltovuori T (2006) Phosphorus in agricultural soils of Finland—characterization of reserves and retention in mineral soil profiles. Pro Terra No. 26. Dissertation, University of Helsinki

Psenner R, Pucsko R, Sager M (1984) Die Fraktionierung organischer und anorganischer Phosphorverbindungen von Sedimenten. Versuch einer Definition ökologisch wichtiger Fraktionen. Fractionation of organic and inorganic phosphorus compounds in lake sediments. An attempt to characterize ecologically important fractions. Arch Hydrobiol Suppl 70:111–155

Reitzel K, Ahlgren J, Gogoll A, Jensen HS, Rydin E (2006) Characterization of phosphorus in sequential extracts from lake sediments using 31P nuclear magnetic resonance spectroscopy. Can J Fish Aquat Sci 63:1686–1699. doi:10.1139/F06-070

Ruttenberg K (1992) Development of a sequential extraction method for different forms of phosphorus in marine sediments. Limnol Oceanogr 37(7):1460–1482

Ruttenberg KC, Berner RA (1993) Authigenic apatite formation and burial in sediments from non-upwelling, continental margin environments. Geochim Cosmochim Acta 57:991–1007. doi:10.1016/0016-7037(93)90035-U

Ruttenberg KC, Goñi MA (1997) Depth trends in phosphorus distribution and C:N:P ratios of organic matter in Amazon Fan sediments: indices of organic matter source and burial history. In: Flood RD, Piper DJW, Klaus A, Peterson LC (eds) Proceedings of the ocean drilling program, scientific results, vol 155, pp 505–517

Salomons W, Gerritse RG (1981) Some observations on the occurrence of phosphorus in recent sediments from western Europe. Sci Total Environ 17:37–49. doi:10.1016/0048-9697(81)90106-6

Schnitzer M (1969) Reactions between fulvic acid, a soil humic compound and inorganic soil constituents. Soil Sci Soc Am Proc 33:75–81

Sholkovitz ER (1976) Flocculation of dissolved organic and inorganic matter during the mixing of river water and seawater. Geochim Cosmochim Acta 40:831–845. doi:10.1016/0016-7037(76)90035-1

Slomp CP, Epping EHG, Helder W, Van Raaphorst W (1996a) A key role for iron-bound phosphorus in authigenic apatite formation in North Atlantic continental platform sediments. J Mar Res 54:1179–1205. doi:10.1357/0022240963213745

Slomp CP, Van der Gaast SJ, Van Raaphorst W (1996b) Phosphorus binding by poorly crystalline iron oxides in North Sea sediments. Mar Chem 52:55–73. doi:10.1016/0304-4203(95)00078-X

Stepanauskas R, Jørgensen NOG, Eigaard OR, Žvikas A, Tranvik LJ, Leonardson L (2002) Summer inputs of riverine nutrients to the Baltic Sea: bioavailability and eutrophication relevance. Ecol Monogr 72(4):579–597

Strom RN, Biggs RB (1982) Phosphorus distribution in sediments of the Delaware River Estuary. Estuaries 5(2):95–101. doi:10.2307/1352106

Sundby B, Gobeil C, Silverberg N, Mucci A (1992) The phosphorus cycle in coastal marine sediments. Limnol Oceanogr 37(6):1129–1145

Suzumura M, Kamatani A (1995) Mineralization of inositol hexaphosphate in aerobic and anaerobic marine sediments: implications for the phosphorus cycle. Geochim Cosmochim Acta 59(5):1021–1026. doi:10.1016/0016-7037(95)00006-2

Uusitalo R (2004) Potential bioavailability of particulate phosphorus in runoff from arable clayey soils. Agrifood Research Reports, 53. Dissertation, University of Helsinki

Vallius H (2006) Permanent seafloor anoxia in coastal basins of the northwestern Gulf of Finland, Baltic Sea. Ambio 35(3):105–108. doi:10.1579/0044-7447(2006)35[105:PSAICB]2.0.CO;2

Van Eck GTM (1982) Forms of phosphorus in particulate matter from the Hollands Diep/Haringvliet, The Netherlands. Hydrobiologia 92:665–681

Virtasalo JJ, Kohonen T, Vuorinen I, Huttula T (2005) Sea bottom anoxia in the Archipelago Sea, northern Baltic Sea. Implications for phosphorus remineralization at the sediment surface. Mar Geol 224:103–122. doi:10.1016/j.margeo.2005.07.010

White RE (1980) Retention and release of phosphate by soil and soil constituents. In: Tinker PB (ed) Soils and agriculture. Critical reports on applied chemistry, vol 2. Blackwell Scientific Publications, Great Britain, pp 71–114

Williams JDH, Syers JK, Walker TW (1967) Fractionation of soil inorganic phosphate by a modification of Chang and Jackson's procedure. Soil Sci Soc Am Proc 31:736–739

Williams JDH, Syers JK, Armstrong DE, Harris RF (1971) Characterization of inorganic phosphate in noncalcareous lake sediments. Soil Sci Soc Am Proc 35:556–561

Williams JDH, Mayer T, Nriagu JO (1980) Extractability of phosphorus from phosphate minerals common in soils and sediments. Soil Sci Soc Am J 44:462–465

Winterhalter B, Flodén T, Ignatius H, Axberg S, Niemistö L (1981) Geology of the Baltic Sea. In: Vopio A (ed) The Baltic Sea. Elsevier oceanography series, 30, Netherlands, pp 1–121